# Supporting Information

# Supermolecular assembly of polyoxoanion and metal-organic cationic units towards model of core–shell nanostructure

Yang-Yang Zhou,[a,†] Ya-jie Kong,[b,†] Qian-Qian Jia,[a] Shuang Yao,*[,a] and Jing-Hui Yan[a]

[a]College of Chemistry and Environmental Engineering, Changchun University of Science and Technology, Changchun, Jilin 130022, P. R. China.

[b] Key Laboratory of Inorganic Chemistry in Universities of Shandong, Department of Chemistry and Chemical Engineering, Jining University, Qufu, Shandong, 273155, P. R. China.

CONTENTS:

## I. Supplementary Structure Figures

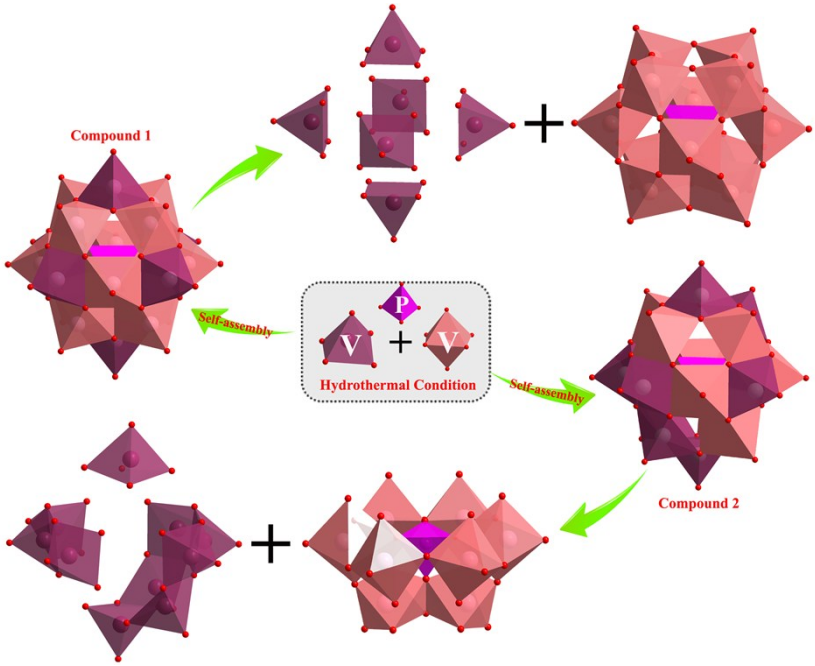


Fig. S1. Two different self-assembly processes in compounds **1** and **2**.

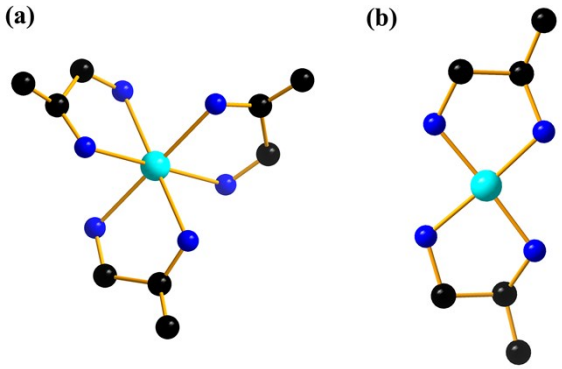


Fig. S2. (a) The hexa-coordinate $[Ni(dap)_3]^{2+}$ in **1** and (b) the tetra-coordinate $[Ni(dap)_2]^{2+}$ in **2**.

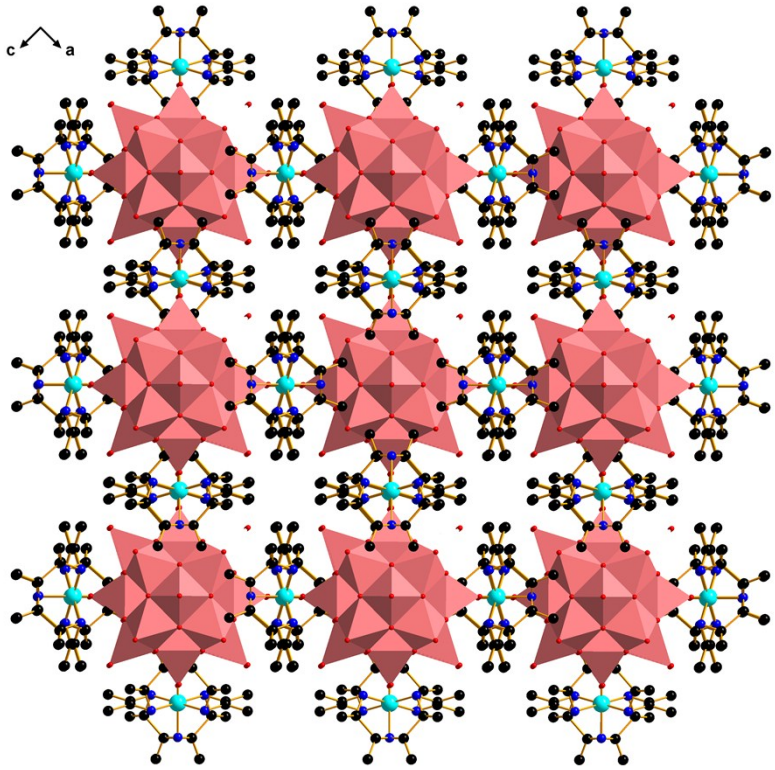


Fig. S3. The 3D supermolecular structure of **1**.

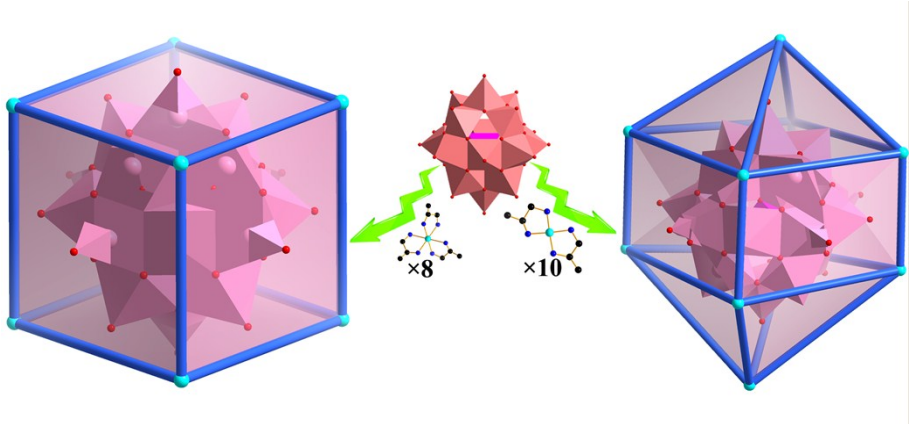


Fig. S4. Scheme view of the POV-based core-shell model composed of different amount of metal-organic units.

## II. Supplementary Experimental Section

IR spectrum was recorded in the range of 400–4000 $cm^{-1}$ on an Alpha Centauri FT/IR Spectrophotometer using KBr pellets. Powder X-ray diffraction (XRD) data were collected by using a Rigaku D/max-2550 diffractometer. The electrochemical measurements were determined by the CHI 600E electrochemical workstation. Platinum gauze was used as counter electrode and Ag/AgCl electrode as reference electrode. A chemically bulk-modified carbon paste electrodes was used as working electrode. The blank carbon paste electrode was prepared by grinding the mixing of 100 mg graphite power and 10 mg compounds **1** and **2** in agate mortar to achieve a uniform mixture, and then two drops of paraffin oil was added with stirring. Then the mixture was transferred to Teflon tube with a 2 mm diameter with firm pressure, and the smooth surface of electrode (**1**-CPE and **2**-CPE).

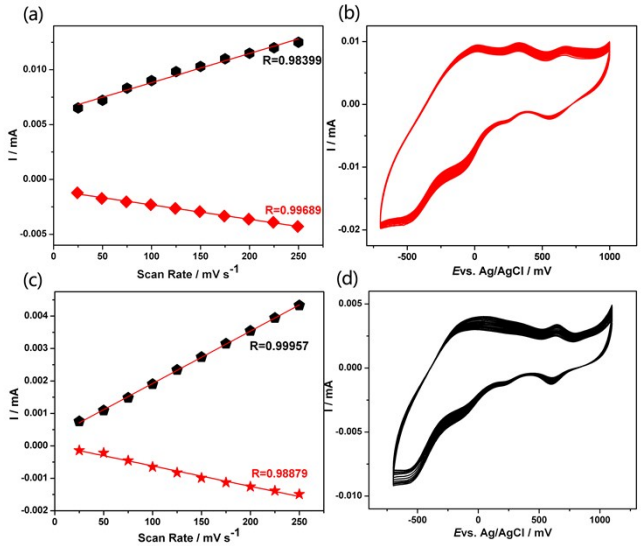


Fig. S5. (a) The corresponding plots of peak current (II and II') of **1**–CPE versus scan rates from 25 to 250 mV $s^{-1}$; (b) CV of the **1**-CPE in 0.2 M $Na_2HPO_4$-$NaH_2PO_4$ buffer solution after 40 repetitive cycles at the scan rate of 100 mV $s^{-1}$; (c) The corresponding plots of peak current (II and II') of **2**–CPE versus scan rates from 25 to 250 mV $s^{-1}$; (d) CV of the **2**-CPE in 0.2 M $Na_2HPO_4$-$NaH_2PO_4$ buffer solution after 40 repetitive cycles at the scan rate of 100 mV $s^{-1}$.

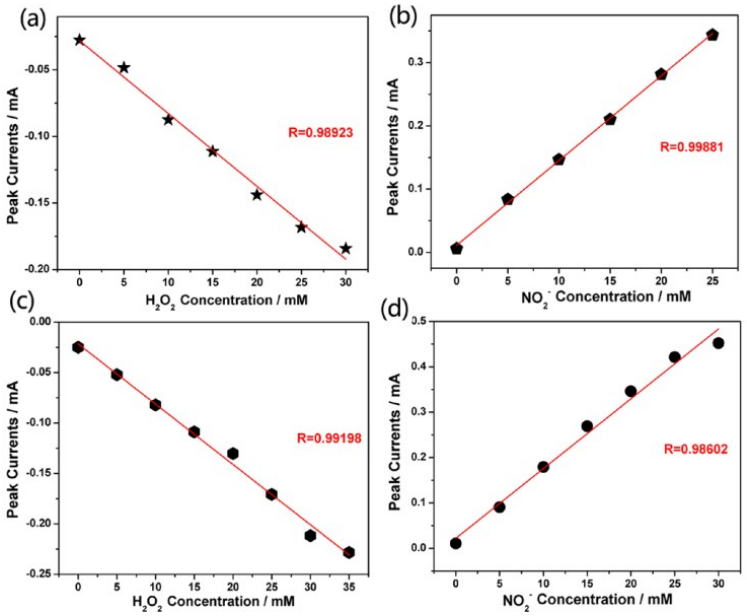


**Fig. S6** The relationship between the peak currents and the concentrations of $H_2O_2$ or $NO_2^-$ with the catalysts **1** (a, b) and **2** (c, d).

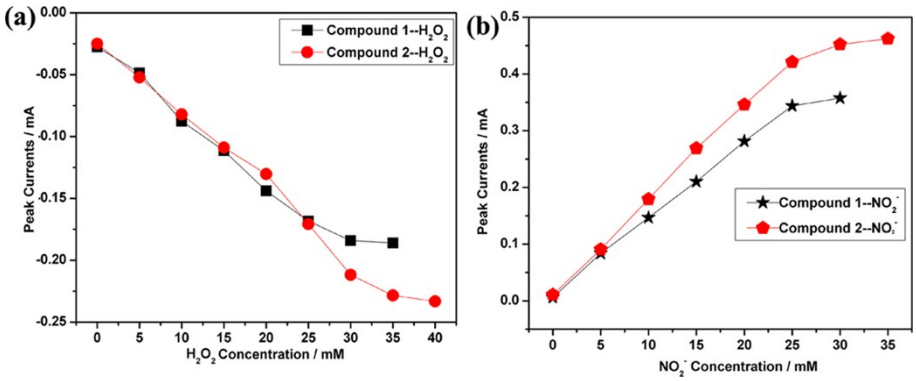


**Fig. S7** The relationship between the peak currents and the concentrations of $H_2O_2$ or $NO_2^-$ with the catalysts **1** and **2**.

Table S1. Bond valence sum calculations of compounds **1** and **2.**[S1,S2]

Compound **1**

| Bonds | Bond Lenth (Å) | BVS | Bonds | Bond Lenth (Å) | BVS |
|---|---|---|---|---|---|
| V(1)-O(4) | 1.621(7) | 1.553546747 | V(4)-O(27) | 1.626(7) | 1.532694085 |
| V(1)-O(5) | 1.958(6) | 0.624833372 | V(4)-O(24)#1 | 1.935(6) | 0.664906993 |
| V(1)-O(5)#1 | 1.958(6) | 0.624833372 | V(4)-O(24) | 1.935(6) | 0.664906993 |
| V(1)-O(6)#1 | 1.986(6) | 0.579293544 | V(4)-O(25)#1 | 1.957(6) | 0.626524395 |
| V(1)-O(6) | 1.986(6) | 0.579293544 | V(4)-O(25) | 1.957(6) | 0.626524395 |
| $V_{V(1)}$ = **3.96** | | | $V_{V(4)}$ = **4.12** | | |
| V(2)-O(10) | 1.602(6) | 1.432554851 | V(3)-O(17) | 1.609(6) | 1.587502715 |
| V(2)-O(11) | 1.904(4) | 0.633334376 | V(3)-O(18) | 1.928(6) | 0.670320046 |
| V(2)-O(14) | 1.920(5) | 0.60653066 | V(3)-O(24) | 1.952(5) | 0.628219994 |
| V(2)-O(6) | 1.965(6) | 0.537072802 | V(3)-O(14) | 1.972(5) | 0.59516362 |
| V(2)-O(9) | 1.965(6) | 0.537072802 | V(3)-O(16) | 2.040(4) | 0.495244993 |
| V(2)-O(3) | 2.433(5) | 0.151603535 | V(3)-O(2) | 2.367(5) | 0.204643367 |
| $V_{V(2)}$ = **4.68** | | | $V_{V(3)}$ = **4.18** | | |
| V(5)-O(26) | 1.607(6) | 1.6984732 | V(7)-O(19) | 1.615(6) | 1.561967034 |
| V(5)-O(22) | 1.907(3) | 0.754967119 | V(7)-O(9) | 1.953(5) | 0.626524395 |
| V(5)-O(23) | 1.934(6) | 0.701837029 | V(7)-O(18) | 1.954(6) | 0.624833372 |
| V(5)-O(20) | 1.938(5) | 0.694290468 | V(7)-O(8) | 1.969(6) | 0.600008888 |
| V(5)-O(25) | 1.973(6) | 0.631624972 | V(7)-O(23) | 1.978(6) | 0.585590151 |
| V(5)-O(1) | 2.469(5) | 0.165298888 | V(7)-O(1) | 2.397(6) | 0.188705521 |
| $V_{V(5)}$ = **4.65** | | | $V_{V(7)}$ = **4.19** | | |
| V(6)-O(12) | 1.607(6) | 1.596107045 | V(8)-O(13) | 1.595(6) | 1.754461833 |
| V(6)-O(7) | 1.912(2) | 0.699942733 | V(8)-O(9) | 1.862(6) | 0.852604532 |
| V(6)-O(8) | 1.920(6) | 0.684971273 | V(8)-O(5) | 1.865(6) | 0.845719472 |
| V(6)-O(20) | 1.938(5) | 0.652445918 | V(8)-O(6) | 1.938(6) | 0.694290468 |
| V(6)-O(5) | 1.945(5) | 0.640218378 | V(8)-O(8) | 1.952(6) | 0.668510816 |
| $V_{V(6)}$ = **4.27** | | | $V_{V(8)}$ = **4.82** | | |
| V(9)-O(15) | 1.607(9) | 1.596107045 | V(10)-O(28) | 1.596(6) | 1.749726447 |
| V(9)-O(14)#1 | 1.872(6) | 0.779853928 | V(10)-O(18) | 1.869(5) | 0.836625802 |
| V(9)-O(14) | 1.872(6) | 0.779853928 | V(10)-O(25) | 1.870(6) | 0.834367705 |
| V(9)-O(11) | 1.985(8) | 0.574615559 | V(10)-O(24) | 1.924(6) | 0.721064255 |
| V(9)-O(16) | 2.135(8) | 0.383099911 | V(10)-O(23) | 1.962(6) | 0.650684932 |
| $V_{V(9)}$ = **4.11** | | | $V_{V(10)}$ = **4.79** | | |
| V(11)-O(21) | 1.634(8) | 1.483782536 | | | |
| V(11)-O(22) | 1.868(8) | 0.788330518 | Ni(1)-N(8)#1 | 1.901(8) | 0.503341463 |
| V(11)-O(7) | 1.886(8) | 0.750897226 | Ni(1)-N(8) | 1.901(8) | 0.503341463 |
| V(11)-O(20)#1 | 1.985(6) | 0.574615559 | Ni(1)-N(7)#1 | 1.909(8) | 0.492575216 |
| V(11)-O(20) | 1.985(6) | 0.574615559 | Ni(1)-N(7) | 1.909(8) | 0.492575216 |
| $V_{V(11)}$ = **4.17** | | | $V_{Ni(1)}$ = **1.99** | | |
| Ni(3)-N(2) | 1.895(9) | 0.511570297 | Ni(2)-N(6)#1 | 1.901(10) | 0.503341463 |

| | | | | | |
|---|---|---|---|---|---|
| Ni(3)-N(1) | 1.899(11) | 0.506069594 | Ni(2)-N(6) | 1.901(10) | 0.503341463 |
| Ni(3)-N(4) | 1.904(9) | 0.499276816 | Ni(2)-N(5)#1 | 1.914(9) | 0.485963568 |
| Ni(3)-N(3) | 1.917(11) | 0.482039253 | Ni(2)-N(5) | 1.914(9) | 0.485963568 |
| $\boldsymbol{V_{Ni(3)}}$ **= 2.00** | | | $\boldsymbol{V_{Ni(2)}}$ **= 1.98** | | |

Compound **2**

| Bonds | Bond Lenth (Å) | BVS | Bonds | Bond Lenth (Å) | BVS |
|---|---|---|---|---|---|
| V(1)-O(2) | 1.587(10) | 1.792809216 | Ni(1)-N(1)#10 | 2.133(13) | 0.31028307 |
| V(1)-O(1)#1 | 1.918(3) | 0.732852511 | Ni(1)-N(1)#11 | 2.133(13) | 0.31028307 |
| V(1)-O(1)#2 | 1.918(3) | 0.732852511 | Ni(1)-N(1)#12 | 2.133(13) | 0.31028307 |
| V(1)-O(1) | 1.918(3) | 0.732852511 | Ni(1)-N(1) | 2.133(13) | 0.31028307 |
| V(1)-O(1)#3 | 1.918(3) | 0.732852511 | Ni(1)-N(1)#13 | 2.133(13) | 0.31028307 |
| V(1)-O(3) | 2.474(10) | 0.163080145 | Ni(1)-N(1)#14 | 2.133(13) | 0.31028307 |
| $\boldsymbol{V_{V(1)}}$ **= 4.89** | | | $\boldsymbol{V_{Ni(1)}}$ **= 1.86** | | |
| V(14)-O(4) | 1.598(14) | 1.635407309 | | | |
| V(14)-O(1) | 1.921(7) | 0.683122499 | | | |
| V(14)-O(1)#8 | 1.921(7) | 0.683122499 | | | |
| V(14)-O(1)#2 | 1.921(7) | 0.683122499 | | | |
| V(14)-O(1)#6 | 1.921(7) | 0.683122499 | | | |
| $\boldsymbol{V_{V(14)}}$ **= 4.37** | | | | | |

## III. Supplementary Characterizations

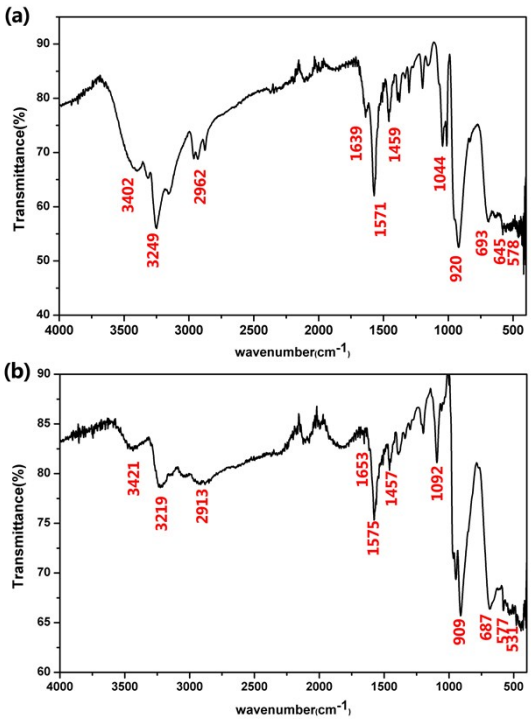


Fig. S8. IR spectra of the compound **1** (a) and compound **2** (b).

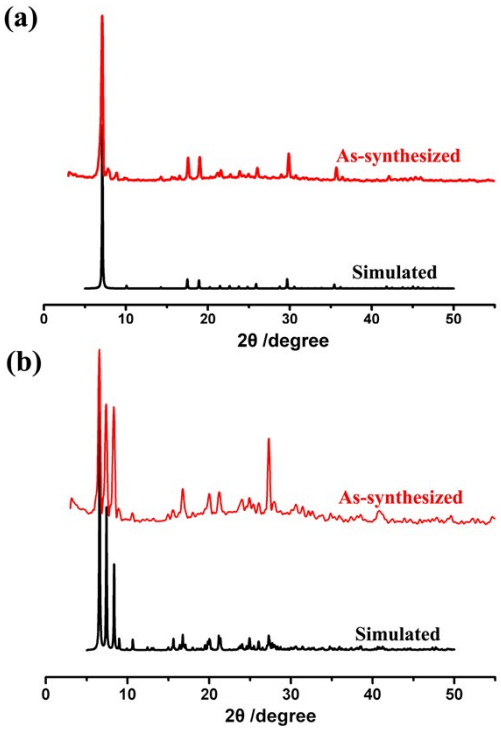


Fig. S9. Comparison of the simulated and experimental PXRD patterns of **1** (a) and **2** (b). The PXRD pattern of as-synthesized samples is identical to the simulated one from the single-crystal X-ray diffraction data, indicating that the single crystal structure is consistent with the bulk sample.

**References**

S1. The valence sum calculations are performed on a program of bond valence calculator, version 2.00 February 1993, written by C. Hormillosa, with assistance from S. Healy, distributed by I. D. Brown.

S2. I. D. Brown, D. Altermatt, *Acta Crystallogr*., 1985, **B41**, 244.